Evolution of bell-shaped dissipative optical solitons from super-gaussian pulse in parabolic law medium with bandwidth limited amplification

SOUMENDU JANA[a,*], SHIVANI[b], GURKIRPAL SINGH PARMAR[a], BALDEEP KAUR[a], QIN ZHOU[c], ANJAN BISWAS[d,e], MILIVOJ BELIC[f]
[a]*School of Physics and Materials Science, Thapar University, Patiala-147004, India*
[b]*Department of Electronics and Communication Engineering, Thapar University, Patiala-147004, India*
[c]*School of Electronics and Information Engineering, Wuhan Donghu University, Wuhan, 430212, P.R. China*
[d]*Department of Mathematical Sciences, Delaware State University, Dover, DE 19901-2277, USA*
[e]*Department of Mathematics, Faculty of Science, King Abdulaziz University, Jeddah-21589, Saudi Arabia*
[f]*Science Program, Texas A & M University at Qatar, Doha, Qatar*

This paper presents evolution of super-Gaussian optical pulses to bell-shaped dissipative solitons in a lossy, cubic-quintic nonlinear (parabolic law) fiber in presence of bandwidth limited amplification. Lagrangian and Rayleigh dissipative function based variational principle leads to a set of evolution equations of individual pulse parameters that determine the condition of stable dissipative soliton pulse propagation. After some initial fluctuations, a flat-top pulse transforms its profile to a bell-shaped one and start propagating in a stable manner. In support of this analytical result, numerical investigations are performed using split-step Fourier method. In this case too, super-Gaussian pulses undergo an initial transition stage before achieving stable bell-shaped solitonic state. Dissipative solitons, thus generated, are found to be robust. This work provides the theoretical backup to experimental procedures of obtaining fundamental soliton from arbitrary pulse using a nonlinear optical fiber.

(Received February 14, 2016; accepted April 5, 2016)

Keywords: Dissipative soliton, Super-Gaussian, Bell-shaped soliton, Cubic-quintic nonlinearity, Frequency-selective feedback

1. Introduction

Optical pulse propagation through nonlinear dispersive media, particularly optical fiber, and eventually the generation of temporal soliton has been at the centre of research interest since its theoretical prediction in 1973 by Hasegawa and Tappert [1]. The interest intensifies after the experimental verification in 1980 by Mollenauer et al. [2]. Temporal soliton is a pulse that preserves its shape and size during propagation. The underlying mechanism is the balancing between linear and nonlinear phenomena. More particularly, the group velocity dispersion (GVD) induced pulse broadening can be arrested by the nonlinearity induced self-phase modulation (SPM) [3]. Temporal soliton, thus generated, has enormous importance in telecommunications, data processing and all-optical devices. In the theoretical study the use of bell-shaped soliton profiles is very common. Among the bell-shaped profiles, either hyperbolic secant (sech) or Gaussian profiles are preferred. It is logical as the sech profile is the exact solution of the cubic nonlinear Schrödinger equation (NLSE) that governs the pulse propagation through nonlinear dispersive media [4]. The Gaussian profile, which is shape wise very close to the sech one, is favourable in many cases as it simplifies the mathematical analysis without much hampering the underlying physics of the system [5]. Also Gaussian pulse gets less influenced by initial chirp in comparison to sech pulse [6]. Apart from these bell-shaped profiles stable temporal soliton has been found with sinh-Gaussian and cosh–Gaussian pulses [7]. Both the pulses have central deep that varies with sinh/ cosh factor. Flat-top pulses are another candidate profile studied in context of temporal soliton in optical fiber [8]. For example, super-Gaussian pulses show stable propagation in an optical fiber [9]. Pulses from directly modulated laser diodes, commonly used in optical fiber communication systems, are far from Gaussian profile. Rather the temporal profile is near-rectangular with steeper edges [10]. Super-Gaussian profile can be suitably assumed for portraying those pulses [11]. The high steepness at the pulse edges significantly modifies SPM, which makes the soliton formation interesting. Apart from the fundamental interest due to their shape these pulses are significant as they can extract more power from the cavity. Super-Gaussian shape is otherwise beneficial as it is less affected by initial linear chirp than Gaussian pulse. Also at higher order with smaller width super-Gaussian pulse can reduce the detrimental effect of timing jitter and bit error rate [12]. The propagation and compression of a broad-band pulse in a chirped-pulse-amplification laser is studied using Super-Gaussian profile [13]. The flat-top nature made super-

Gaussian pulses versatile and suitable for use, e.g., high-energy ion acceleration. The proton acceleration in the interaction of a tightly focused pulse with ultrathin double-layer solid targets in the regime of directed Coulomb explosion significantly increases using super-Gaussian pulses [14]. These pulses have been used in the study of long-range self-channelling of infrared laser pulses in air [15]. To get a better insight into the mechanism preventing long-range beam collapse, numerical simulations were performed considering a super-Gaussian beam profile that matches with the experimental beam. Alongside of Gaussian profile super-Gaussian profile has been employed in designing optical devices and systems. For instance, it has been used to find optimal pump profiles to improve the delay performance of tunable, broadband, slow-light pulse delay devices based on stimulated Brillouin scattering [16]. Super-Gaussian profile is often sought after as an approximation of square / rectangular pulse profiles. It has been considered in place of commonly used square pulses in non-return-to-zero systems in designing fiber grating filters in dense wavelength-division multiplexed systems. [17].

The nonlinear propagation of super-Gaussian pulse mostly studied in Kerr media. In optical fiber Kerr /cubic nonlinearity is the most prominent nonlinearity. At moderately higher intensity in semiconductor doped fiber nonlinearity gets modified. This can be modelled by adding quintic term with cubic (Kerr) nonlinearity. Although its value is very small in comparison to Kerr one, it significantly modifies pulse propagation, self-focusing, soliton condition and other related optical phenomena. Also quintic nonlinearity initiates some optical phenomena which are absent in solely cubic nonlinearity environment [18-20].

The theoretical investigation on the propagation of super-Gaussian optical pulses is carried by both numerically and analytically. A direct numerical simulation shows that super-Gaussian profile turns to two-peak and, finally, to single-peak while propagating through a dispersive single mode fiber [21]. Also, the peak intensity increases initially and then decreases monotonically after reaching a maximum. However, this decay can be arrested in nonlinear media, which will be demonstrated in the current communication. Using Runge-Kutta method it has been shown that pulse width and frequency chirp oscillate with the increasing distance if normalized coefficient of the second-order dispersion is appropriate and initial chirp is sufficiently small [22]. Also frequency-jitter and phase increases with propagation. The condition of conformal transmission of super-Gaussian pulse in optical fibers has been derived. Attempt has been made to achieve Super-Gaussian solitons in dispersion-managed optical fibers with perturbation using variational method [23]. However, it only presents the evolution equations (that are too in implicit form) of the pulse parameters during propagation. There is scope of further analysis of those equations, which essentially gives better insight about the pulse dynamics in the perturbed system. Using variational method solitons of super- Gaussian shape have been found in semiconductor doped glass fibers that possess cubic-quintic nonlinearity. Stability analysis proved that these solitons are dynamically stable and robust against small perturbation [24]. Also super-Gaussian shaped dispersion-managed solitons in polarization preserving optical fibers are obtained. In this study cubic nonlinearity is considered in conjugation with both local and non-local perturbation terms [25].

A real time optical fiber will be always associated with some loss, whatever small it is. To compensate the loss, a suitable gain is essential. Only when GVD-SPM and gain-loss balances are achieved a soliton can be formed. Such soliton is called as dissipative soliton due to the dissipative nature of the host system. In this communication we present super-Gaussian pulse propagation and subsequent evolution as a bell-shape dissipative soliton in a lossy optical fiber having cubic-quintic (parabolic law) nonlinearity. To provide the continuous supply of gain to the lossy system we use bandwidth limited amplification. For this a frequency-selective optical feedback is coupled with the fiber. An experimentalist's way to obtain a fundamental soliton of sech shape from an arbitrary pulse is to let the arbitrary pulse transmit through a nonlinear optical fiber. In the due course after radiating excess energy and balancing of dispersion-nonlinearity phenomena the fundamental soliton emerges. Present communication aims to provide the theoretical support of such experiments in a real time, lossy, nonlinear fiber.

The arrangement of this paper is as follows: the mathematical model, which is a perturbed nonlinear Schrödinger equation, is described in section 2. The evolution equations of the pulse parameters are obtained by perturbative variational method. Result of analytical method and the condition for dissipative soliton formation is discussed in section 3. Also, the variationally obtained solitons are validated by the direct numerical simulation based on split step Fourier transformation (SSFT). A brief conclusion is presented in section 4.

2. Mathematical model

To study the propagation dynamics of the super-Gaussian pulse in a lossy optical fiber with cubic-quintic (parabolic law) nonlinearity and bandwidth limited amplification (by means of frequency-selective feedback) we consider the following cubic-quintic nonlinear Schrödinger equation (CQNLSE):

$$i\frac{\partial U}{\partial z}+\frac{d(z)}{2}\frac{\partial^2 U}{\partial T^2}+|U|^2U+\gamma|U|^4U = \frac{i}{2}(g_0-\alpha)U+i\beta\frac{\partial^2 U}{\partial T^2} \tag{1}$$

where, z is normalized distance of propagation, T is retarded time, $U(z)$ is the slowly varying envelope of the electric field of the pulse, $d(z)$ is the dispersion. In eq.(1)

the first term represents the evolution of the pulse field with respect to z, second one is the GVD term, while the third and forth terms are the contribution due to cubic and quintic nonlinearity respectively. γ measures the strength of quintic nonlinearity relative to cubic one, thus have very small value. We consider negative value of γ, which means the quintic nonlinearity is of defocusing nature. This combination of positive (focusing) cubic and negative quintic (defocusing) nonlinearity is a kind of competing nonlinearity that promises intriguing pulse dynamics. The lossy nature of the system is represented by the loss coefficient α, g_0 is the coefficient of gain supplied in the system by optical frequency-selective feedback. Frequency-selection is done by the help of a filter of strength β that yields the last term [26]. The two terms together on the right hand side of (1) is known as bandwidth limited amplification. Eq.(1) can be rewritten as a perturbed CQNLSE of following form:

$$i\frac{\partial U}{\partial z}+\frac{d(z)}{2}\frac{\partial^2 U}{\partial T^2}+|U|^2U+\gamma|U|^4U=iR \quad (2)$$

The right hand side of eq.(1) represents perturbation in the fiber, with $R=\delta U+\beta\frac{\partial^2 U}{\partial T^2}$ Here, $\delta=(g_0-\alpha)/2$ measures the excess gain that can further compensate the detrimental effect of the filter. A number of analytical methods have been developed for decades to solve NLSE. The most successful methods are inverse scattering method, Lax pair method, AKNS method, Fourier series method, Bäcklund transformation method, Darboux transformations technique and Green function technique. The objective of these methods is to check the integrability and subsequently find the exact solution of the system. Indeed presence of perturbation in NLSE more accurately describes the pulse dynamics in a real fiber but invites complexity in solving the problem as well. Solving eq. (1) by the aforesaid 'exact' analytical methods is difficult as this type of perturbed NLSE are in general non-integrable. In fact, equation (1) with dissipative perturbation terms that render any nonlinear evolution is non-integrable. There are several algorithms that are applicable if the perturbation terms are Hamiltonian. They are ansatz approach, semi-inverse variational principle. These have been successfully applied in the past [27-33]. Additionally, multiple-scale perturbation technique has been successfully applied to secure approximate soliton solution to the perturbed system. Another means to address such perturbed system where the perturbation terms are non-Hamiltionian is the variational principle [34, 35], as being studied in this paper. It must be noted that this principle does not yield a solution to the governing equation. It only retrieves dynamical system to the parameters of the soliton in presence of perturbation terms.

For non-integrable models, approximate analytical methods are in rescue. We adopt Lagrangian based variational method in conjugation with Rayleigh dissipative function to find the evolution of the pulse parameters with propagation distance [26, 36]. Also, it should be noted that we are not searching the standard soliton solution of fundamental or higher order, rather investigating the propagation behaviour and checking the possibility of generating soliton from a given form (here, super-Gaussian) of pulse. The freedom of choosing ansatz other than the exact one is the indispensable reason to select variational method. Although approximate, this method is a very strong and useful toll to predict the nonlinear dynamics of pulse and beam even in perturbed environment [26]. To start with we first consider the unperturbed part of eq.(2), i.e.,

$$i\frac{\partial U}{\partial z}+\frac{d(z)}{2}\frac{\partial^2 U}{\partial T^2}+|U|^2U+\gamma|U|^4U=0 \quad (3)$$

The Lagrangian density for this part reads as

$$\begin{aligned}L&=\frac{i}{2}(U^*U_Z-UU_Z^*)\\&-\frac{d(z)}{2}|U_T|^2+\frac{1}{2}U^4+\frac{\gamma}{3}U^6\end{aligned} \quad (4)$$

At this point it is necessary to introduce a trial function, which is the pulse profile under investigation [37]. For the conservative CQNLSE (eq. 3) we neither consider the exact soliton ansatz of the pioneering paper by Pushkarov et.al. [38] nor the 'inverse cosh' type variational ansatz by de Angelis [34]. Since our aim is to study the propagation dynamics and to test the possibility of getting soliton (whatever the shape is) from a super-Gaussian pulse, we consider the following form of super-Gaussian trial function:

$$\begin{aligned}U(z,T)&=A(z)\exp\left\{-\left[P(z)(T-T_0(z))\right]^{2m}\right\}\\&\times\exp\left[i\begin{Bmatrix}c(z)(T-T_0(z))^2\\-k(z)(T-T_0(z))+\sigma(z)\end{Bmatrix}\right]\end{aligned} \quad (5)$$

Here, $A(z)$ represent the pulse amplitude, $P(z)$ is the inverse pulse width, $T_0(z)$ is the pulse centre and $c(z)$ is the chirp. $k(z)$ and $\sigma(z)$ respectively capture the nonlinear frequency shift and phase of the soliton pulse. m is the super-Gaussian parameter that decides the flatness of the pulse. With increasing value of m the pulse gets flatter as well as pulse edge becomes steeper. Inserting this trial function in the Lagrangian eq.(4) and integrating over the entire time zone we get the total Lagrangian as:

$$<L>\int_{-\infty}^{+\infty}LdT \quad (6)$$

$$< L >= \frac{A^2 k\theta(m)}{2^{\frac{1}{2m}} p}\frac{dT_0}{dz} - \frac{A^2\theta(m)}{2^{\frac{1}{2m}} p}\frac{d\sigma}{dz} - \frac{A^2 dk^2\theta(m)}{2^{1+\frac{1}{2m}} p} - \frac{A^2\beta_c(m)}{2^{\frac{3}{2m}} p^3}\frac{dc}{dz} - \frac{2A^2 dc^2\beta_c(m)}{2^{\frac{3}{2m}} p^3} - \frac{2^{\frac{1}{2m}} A^2 m^2 Pd\eta(m)}{2}\frac{d\sigma}{dz} + \frac{A^4\theta(m)}{2^{1+\frac{1}{2m}} p} + \frac{\gamma A^6\theta(m)}{3.(6)^{\frac{1}{2m}} p} \quad (7)$$

where, $\theta(m) = \frac{1}{m}\Gamma(1/2m)$, $\beta_c(m) = \frac{1}{m}\Gamma(3/2m)$, $\eta(m) = \frac{1}{m}\Gamma((4m-1)/2m)$ and $\Gamma(x)$ is the gamma function. We use the following Eular-Lagrangian equation for the variation of total Lagrangian.

$$\frac{\partial < L >}{\partial r_j} - \frac{d}{dz}\left(\frac{\partial < L >}{\partial(\frac{\partial r_j}{\partial z})}\right) = i\int_{-\infty}^{+\infty}\left(R\frac{\partial U^*}{\partial r_j} - R^*\frac{\partial U}{\partial r_j}\right)dT \quad (8)$$

where, r_j stands for the pulse parameters namely A, P, c, T_0, k and σ. Variation with respect to these six parameters yields following six equations that show the evolution of the pulse parameters during propagation.

$$\frac{dk}{dz} = -2^{2+\frac{1}{m}} m^2 k\beta P^2\left(\frac{\eta(m)}{\theta(m)}\right) - \frac{2^{4-\frac{1}{m}}\beta c^2 K}{P^2}\left(\frac{\beta_c(m)}{\theta(m)}\right) \quad (9)$$

$$\frac{dA}{dz} = -Acd + A(\delta - k^2\beta) - \frac{3m(2m-1)\beta AP^2}{2^{1-\frac{1}{m}}}\left(\frac{\lambda(m)}{\theta(m)}\right) + \frac{3m\beta AP^2}{2^{1-\frac{1}{m}}}\left(\frac{\eta(m)}{\theta(m)}\right) - \frac{2^{m-3}\beta AP^2}{2^{3-\frac{1}{m}}}\left(\frac{\beta_c(m)}{\theta(m)}\right) + \frac{2^{1-\frac{1}{m}}\beta Ac^2}{P^2}\left(\frac{\mu(m)}{\beta_c(m)} - \frac{3\beta_c(m)}{\theta(m)}\right) \quad (10)$$

$$\frac{dP}{dz} = -2dcP + \frac{(2m-3)\beta P^3}{2^{2-\frac{1}{m}}}\left(\frac{\theta(m)}{\beta_c(m)}\right) - 2^{\frac{1}{m}} m(2m-1)\beta P^3\left(\frac{\lambda(m)}{\theta(m)}\right) + 2^{\frac{1}{m}} m^2\beta P^3\left(\frac{\eta(m)}{\theta(m)}\right) + \frac{2^{2-\frac{1}{m}}\beta c^2}{P}\left(\frac{\mu(m)}{\beta_c(m)} - \frac{\beta_c(m)}{\theta(m)}\right) \quad (11)$$

$$\frac{dT_0}{dz} = -kd + \frac{2^{3-\frac{1}{m}}\beta ck}{P^2}\left(\frac{\beta_c(m)}{\theta(m)}\right) \quad (12)$$

$$\frac{dc}{dz} = 2^{\frac{2}{m}-1} m^2 dP\left(\frac{\eta(m)}{\beta_c(m)}\right) - 2dc^2 - \frac{A^2P^2}{2^{2-\frac{1}{2m}}}\left(\frac{\theta(m)}{\beta_c(m)}\right) - \frac{2^{\frac{1}{m}}\gamma A^4P^2}{3^{1+\frac{1}{2m}}}\left(\frac{\theta(m)}{\beta_c(m)}\right) - 2^{1+\frac{1}{m}} m\beta cP^2\left(\frac{\theta(m)}{\beta_c(m)}\right) \quad (13)$$

and

$$\frac{d\sigma}{dz} = \frac{k^2 d}{2} - 2^{\frac{1}{m}} m^2 dP^2\left(\frac{\eta(m)}{\theta(m)}\right) + \frac{5A^2}{2^{2+\frac{1}{2m}}} + \frac{4\gamma A^2}{3^{1+\frac{1}{2m}}} - \frac{2^{3-\frac{1}{m}}\beta ck^2}{P^2}\left(\frac{\beta_c(m)}{\theta(m)}\right) + 2m\beta c \quad (14)$$

Here, $\lambda(m) = \frac{1}{m}\Gamma((2m-1)/2m)$ and $\mu(m) = \frac{1}{m}\Gamma(5/2m)$. These equations are further solved to determine the pulse dynamics. Eq.(9) –(14) reduce to their unperturbed evolution equations by setting $\delta = \beta = 0$.

3. Results and discussions

To achieve the stable solitonic pulse dynamics first we have to find the set of nontrivial stationary points. By setting left hand sides of eq. (9) – (14) to zero and solving the resultant equations one can get the set of stationary points. But, unlike unperturbed case explicit expressions of the stationary points in perturbed case are too tricky to determine due to the complex nature of the equations. Therefore, we find them graphically. For some given value of γ, β, d and δ, we fix values of A and k to plot P versus c curves for different m values. Any point on the curve (P_S, c_S), in conjugation with the already fixed points, will be a set of stationary points. In Fig. 1 stationary points are plotted for two different strength of quintic nonlinearity for different value of super-Gaussian parameter m. The higher the value of m, the lower the value of P_S for a given set of c_S and γ. The behaviour of the stationary points is similar for different strength of quintic nonlinearity

(γ). However, for a higher value of $|\gamma|$, P_S will be smaller for a given value of c_S. This is more prominent at lower values of c_S. This way of finding stationary points is a privilege to experimentalist as with a given set of system parameter a large family of stationary points can be obtained using such plots for any given strength of nonlinearity. These stationary points from Fig. 1 are considered as the initial values of the corresponding parameters to solve the evolution equations of the pulse parameters, i.e., eq. (9)–(14) following Range-Kutta method. Fig. 2 (a) shows the variation of k, A, c and P with propagation distance for $m=1$. k remains constant throughout the propagation, while A, c and P show an initial fluctuating region about their respective stationary values. Subsequently, the oscillations stabilize and steady state is achieved. The origin of the oscillatory initial phase is worthy to be found out. It is known that an incident pulse of other than the exact soliton shape transforms to the soliton shape while propagating. Variational method is believed to be unsuccessful to capture this transformation. In contrary, in Fig. 2 (a) the fluctuation seems to be the indication of the aforesaid shape changing of the pulse. The role of phase plots in nonlinear dynamics is inevitable. They are very useful for determining the dynamical nature of the system as well as classifying the equilibrium points.

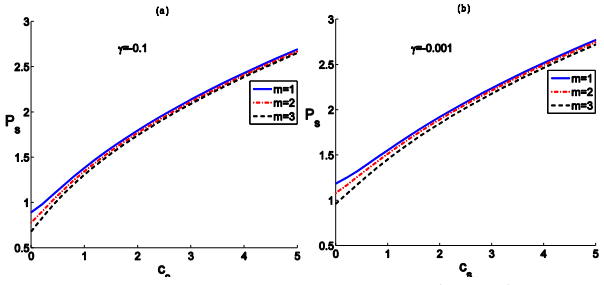

Fig. 1. Behaviour of stationary points (P_S, c_S) *with* m *as a parameter.* $A=1$, $d=1$, $k=0$, $\delta=0.04$ *and* $\beta=0.15$. *(a)* $\gamma-0.1$. *(b)* $\gamma-0.001$.

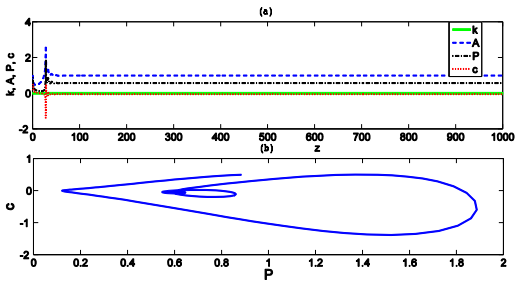

Fig. 2. (a) Evolution of steady state solitonic pulse parameters after an initial fluctuation of those of a super-Gaussian ($m=1$ *) pulse, in presence of perturbation. (b)The phase plot corresponding to Fig. 2(a) showing bound state propagation. For both of the figures* $A=1$, $d=1$, $k=0$, $\delta=0.04$, $\beta=0.15$ *and* $\gamma-0.001$

Here, phase plot corresponding to Fig. 2(a) has been depicted in Fig. 2(b). The phase trajectory is having counter clockwise spiral motion that finally ends at a point. This suggests stable focus, i.e., the bound state forming an attractor. Evolution of k, A, c and P with propagation distance for $m=2$ and 3 have been depicted in Fig. 3(a) and Fig. 4(a) respectively. Corresponding phase plots are presented in Fig. 3(b) and Fig. 4(b) respectively. For both values of m pulse parameters overcome the initial fluctuations to achieve a steady state. At this point it is worthy to clarify the difference between our results (presented in Fig. 2(a), 3(a) and 4(a)) and that demonstrated in ref [25]. In ref [25] stationary points are determined in absence of perturbation and hence the pulse parameters show steady state propagation. Then small arbitrary perturbation is added to the values corresponding to the stationary points and the pulse parameters started oscillating periodically around the stationary points. That means the use of perturbation is to establish the robustness of the system.

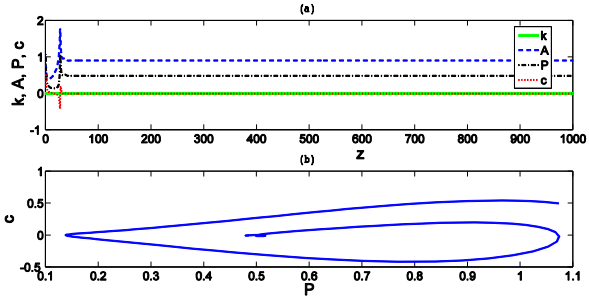

Fig. 3. (a) Initial shape transforming fluctuation of super-Gaussian ($m=2$ *) pulse parameters and subsequent steady state variation in presence of perturbation. (b) The phase plot corresponding to Fig. 3 (a) showing bound state propagation. The values of* A, d, k, δ, β *and* γ *are same as Fig. 2.*

But our present model manages to keep one step ahead by including meaningful dissipative terms as perturbation to acquire better insight of the system dynamics. This in turn enables the said model suitable for investigating dissipative solitons.

We found stationary points, thanks to variational method, for the perturbed system itself. Consequently the pulse parameters in Fig. 2, 3 and 4 evolve to steady state after some initial shape changing turbulence. These self-localized pulses can be referred as dissipative solitons. Point to be noted that although we used constant dispersion for plotting, our model contains a variable dispersion $d(z)$. Such dispersion map may be investigated elsewhere.

To validate the analytical results a direct numerical solution of eq. (1) is in order now. We adopted split-step Fourier transformation method (SSFM) to solve eq. (1) with the analytically determined stationary points (from Fig. 1) as initial conditions. Fig. 5(a) shows the pulse evolution for $m=1$. Corresponding contour plot is presented in Fig. 5 (b). Both the plots show that after an initial shape adjustment the incident pulse quickly attains bell-shaped solitonic shape and then executes steady state propagation.

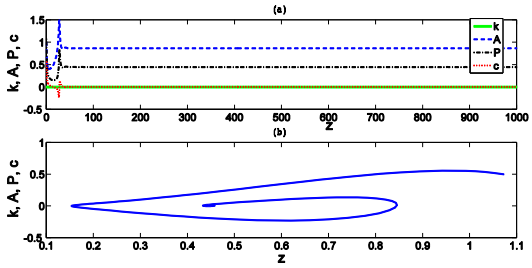

Fig. 4. (a) Initial shape transforming fluctuation of super-Gaussian pulse ($m=3$) and subsequent steady state variation in presence of perturbation. (b) The phase plot corresponding to Fig. 4(a) showing bound state propagation. The values of A, d, k, δ, β and γ are same as Fig. 2.

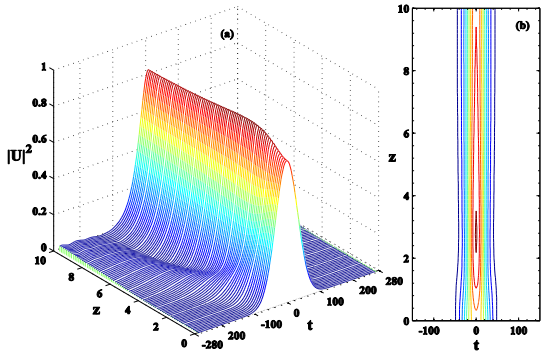

Fig. 5. (a) Evolution of super-Gaussian pulse ($m=1$) to a bell-shaped dissipative soliton. The values of A, d, k, δ, β and γ are in accordance with those of Fig. 2. (b). The corresponding contour plot.

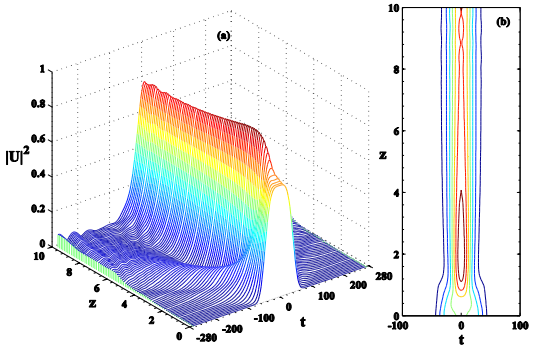

Fig. 6. Generation of bell-shaped dissipative soliton with super-Gaussian ($m=2$) pulse. The values of A, d, k, δ, β and γ are in accordance with those of Fig. 3.

Figs. 6 and 7 portray the evolution of high order super-Gaussian pulses (respectively for $m=2$ and 3) under the effect of perturbation. Higher order super-Gaussian pulses, which are of flat-top profiles, first transform to bell-shaped profile and thereafter propagate as steady state soliton. For a given value of d greater δ is required to achieve a stable soliton from higher order super-Gaussian pulse. This is reasonable as higher order pulse possesses more energy and hence requires more gain for soliton generation. The reshaping of incident pulse to a solitonic profile is accomplished by the radiation of excess energy, which is prominent for all three super-Gaussian case. The greater the super-Gaussian parameter, i.e., greater the difference with solitonic shape, the higher the radiation. Finally, both the analytical and numerical results qualitatively agree to the fact that super-Gaussian pulses, after an initial transition phase, are able to generate stable solitons. Importantly, variational method went above and beyond the usual results by capturing the initial shape transformation of super-Gaussian pulses.

At this point perhaps it may not be irrelevant to discuss why the flat-top profile could not be preserved in an optical fiber. Getting soliton of super-Gaussian or flat-top profile is not very common. The geometry of bulk media plays a hand in achieving the flat-top soliton. One may get flat-top soliton by supplying huge nonlinear gain (e.g., cubic) and other dissipative terms in the system as in case of ref. [39, 40]. Also flat-top soliton may be achieved in optical lattices by stabilizing multi-soliton complex [41], or by coherent pulse stacking in a multicrystal (10-crystal fan) birefringent filter [42]. A flat-top soliton can also be excited from cosh-Gaussian beam, which is again combination of two decentered Gaussian beams, in defocusing quintic nonlinear media only at high power [43]. In optical fiber very strong dissipation and line gain may lead to flat-top profile [44]. In the references [39-44] the flat-top profile is obtained starting from some non-flat-top profile. Since our scheme does not involve a broad area or bulk device, doesn't have nonlinear gain or very high dissipation term and we are not putting very high power in the fiber we should not be optimistic to get a flat-top soliton.

Finally, the robustness of the dissipative solitons thus generated can be verified by setting initial conditions around the stationary values (given by Fig. 1). For the said case super-Gaussian pulses of all three orders evolve to periodically oscillating bell-shaped solitons. This is depicted in Fig. 8 for super-Gaussian pulse with $m=1$, 2 and 3.

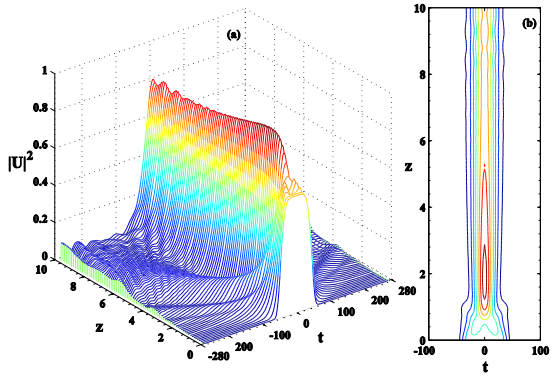

Fig. 7 Evolution of super-Gaussian pulse ($m=3$) and generation of a bell-spaped dissipative soliton. The values of A, d, k, δ, β and γ are in accordance with those of Fig. 4.

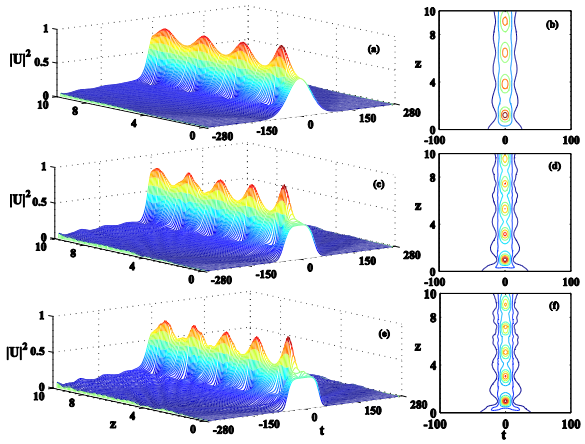

Fig. 8. Generation of periodically oscillating bell-shaped solitons from super-Gaussian pulses. For (a) and (b) $m=1$, for (c) and(d) $m=2$, for (e) and(f) $m=3$. Initial conditions are slightly different from the steady state pulse parameters obtained from Fig. 1.

4. Conclusion

In this paper, we investigated the propagation of Super-Gaussian optical pulse and subsequent evolution of bell-shaped dissipative soliton in cubic-quintic (parabolic law) lossy medium in presence bandwidth limited amplification due to frequency-selective feedback. Variational method in conjugation with Rayleigh dissipative function is used to derive a set of evolution equations of pulse parameters. The condition of steady state solitonic pulse propagation is derived. A large family of system parameters has been identified that promises stable dissipative soliton. SSFM based numerical experiments are performed with super-Gaussian optical pulses. Both the analytical and numerical results show that initially there are some shape transforming fluctuations in pulse parameters and then the pulses evolve as stable dissipative solitons. Although, higher order super-Gaussian pulses do not preserve their characteristic flat-top profile, they evolve as bell-shaped dissipative soliton. Therefore, a solitonic pulse can be achieved in dissipative media from pulses having flat-top or other steep edged profiles, e.g., radiation from directly modulated laser diodes that is commonly used in fiber optic communication systems. The result can be used in data communications, all-optical switching, and signal processing.

Acknowledgement

Baldeep Kaur would like to acknowledge the financial support of UGC, Govt. of India, through UGC Meritorious Scholarship. Gurkirpal Singh Parmar would like to acknowledge TEQUIP for financial assistance. The research work of last two authors (Anjan Biswas and Milivoj Belic) was funded by Qatar National Research Fund (QNRF) under grant number NPRP 6-021-1-005. The authors also declare that there is no conflict of interest.

References

[1] A. Hasegawa, F. Tappert, Appl. Phys. Lett. **23**, 142 (1973).
[2] L. F. Mollenauer, R. H. Stolen, J. P. Gordon, Phys. Rev. Lett. **45**, 1095 (1980).
[3] G. P. Agrawal, Nonlinear Fibre Optics 3rd edn, Academic press: Berlin (2011).
[4] N. Akhmediev, A. Ankiewicz, Dissipative Solitons, Springer, Berlin, (2005).
[5] P. Lazaridis, G. Debarge, P. Gallion, Opt. Lett. **20**, 1160 (1995).
[6] T. Kacmarek, Mod. Probl. of Radio Eng., Telecommun. and Computer Sci.: Proceedings of the International Conference, 105, (2004).
[7] S. Konar, S. Jana, Opt. Commun. **236**, 7 (2004).
[8] E. Palushani, L. K. Oxenløwe, M. Galili, H. C. Mulvad, A. T. Clausen, P. Jeppesen, IEEE J. of Quant. Electron. **45**, 1317 (2009),
[9] D. Anderson, M. Lisak, Opt. Lett. **11**, 569 (1986).
[10] R. A. Linke, IEEE J. Quant. Electron. **21**, 593 (1985).
[11] G. P. Agrawal, M. J. Potasek, Opt. Lett. **11**, 318 (1986).
[12] M. Singh, A. K. Sharma, R. S. Kaler, Optik, **121**, 609 (2010).
[13] Y. H. Chuang, L. Zheng, D. D. Meyerhofer, IEEE J of Quant. Electron. **29**, 270 (1993).
[14] S. S. Bulanov, A. Brantov, V. Y. Bychenkov, V. Chvykov, G. Kalinchenko, T. Matsuoka, P. Rousseau, S. Reed, V. Yanovsky, D. W. Litzenberg, K. Krushelnick, A. Maksimchuk, Phys. Rev. E **78**, 026412 (2008).
[15] G. M´echain, A. Couairon, Y. B. Andr´e, C. D'amico, M. Franco, B. Prade, S. Tzortzakis, A. Mysyrowicz, R. Sauerbrey, Appl. Phys. B 79, 379 (2004).
[16] R. Pant, M. D. Stenner, M. A. Neifeld, D. J. Gauthier, Opt. Express **16**, 2764 (2008).
[17] B. J. Eggleton, G. Lenz, N. Litchinitser, D. B. Patterson, R. E. Slusher, IEEE Photon. Technol. Lett. **9**, 1403 (1997).
[18] P. Roussignol, D. Ricard, J. Lukasik, C. Flytzanis, J. Opt. Soc. Am. B **4**, 5 (1987).
[19] J. Coutaz, M. Kull, J. Opt. Soc. Am. B **8**, 95 (1991).
[20] J. Soneson, A. Peleg, D. Physica, Nonlinear Phenomena **195**, 123 (2004).
[21] S. Konar, S. Jana, Phys. Scr. **71**, 198 (2005).
[22] G. Xia, Z. Wu, J. Wu, Chin. J. Phys. **41**, 116 (2003).
[23] L. Miao, X. Xu-ming, Y. Chun-yun, Y. Tao, Chin. J. Quantum Electron. **28**, 369 (2011).
[24] A. Biswas, Fiber and Integr. Opt **21**, 115 (2002).
[25] Shwetanshumala, A. Biswas, S. Konar, J. Electromagn. Waves Appl. **20**, 901 (2006).
[26] R. Kohl, D. Milovic, E. Zerrad, A. Biswas, Mathematical and Computer Modelling **49**, 1700 (2009).
[27] A. Biswas, J. Opt. A **4**, 84 (2002).
[28] P. Green, D. Milovic, A. K. Sarma, D. A. Lott, A.

Biswas, J. Nonlin. Opt. Phys. Materials **19**, 339 (2011).
[29] A. H. Bhrawy, M. A. Abdelkawy, A. Biswas, Optik **125**, 1537 (2014).
[30] A. H. Bhrawy, A. A. Alshaery, E. M. Hilal M. Savescu, D. Milovic, K. R. Khan, M. F. Mahmood, Z. Jovanoski, A. Biswas, Optik **125**, 4935 (2014).
[31] A. H. Bhrawy, A. A. Alshaery, E. M. Hilal, K. R. Khan, M. F. Mahmood, A. Biswas, Optik **125**, 4945 (2014).
[32] A. A. Alshaery, A. H. Bhrawy, E. M. Hilal, A. J. Biswas, Electromag. Waves and Applic. **28**, 275 (2014).
[33] A. H. Bhrawy, A. A. Alshaery, E. M. Hilal, D. Milovic, L. Moraru, M. Savescu, A. Biswas, Proc. Roman. Acad. **15**, 235 (2014).
[34] C. De Angelis, IEEE J. Quant. Elect. **30**, 818 (1994).
[35] A. Biswas, A. B. Aceves, J. Mod. Opt. **48**, 1135 (2001).
[36] A. Hasegawa, Pramana **57**, 1097 (2001).
[37] D. Anderson, Phys. Rev. A **27**, 3135 (1983).
[38] Kh. I. Pushkarov, D. I. Pushkarov, I. V. Tomov, Opt. Quant. Electr. **11**, 471 (1979).
[39] P. Grelu, N. Akhmediev, Nat. Photon. **6**, 1 (2012).
[40] L. C. Crasovan, B. A. Malomed, D. Mihalache, Phys. Lett. A **289**, 59 (2001).
[41] T. J. Alexander, Y. S. Kivshar, Appl. Phys. B **82**, 203 (2006).
[42] I. Will, G. Klemz, Opt. Exp. **16**, 14922 (2008).
[43] S. Konar, M. Mishra, S. Jana, Phys. Lett. A **362**, 505 (2007).
[44] X. Liu, Opt. Exp. **19**, 5874 (2011).

*Corresponding author: soumendujana@yahoo.com